Application of Probabilistic Modelling to the Lifetime Management of Nuclear Boilers in the Creep Regime: Part 1

by P.J.Holt[1] and R.A.W.Bradford[2]
[1]Veritan Ltd, 4 Valley View, Lower Mills, Stonehouse, Glos.GL10 2BB, peter.holt@veritan.co.uk
[2]EDF Energy, Barnett Way, Barnwood, Glos.GL4 3RS, rick.bradford@edf-energy.com

Abstract

Monte Carlo probabilistic simulation has been applied to a large population of nominally identical components in an AGR boiler operating in the creep regime. The components have a history of defectiveness. The R5 procedure is used to calculate creep-fatigue crack growth rates within a probabilistic programme. The inspection process is also modelled probabilistically. The overall result is a 'prediction' of past inspection results which can be used to tune the parameters of the model. The model then makes genuine predictions of the required level of remediations in future overhauls by predicting the inspection results. The probabilistic treatment of both the structural calculations and the inspection process jointly has been shown to assist in clarifying the interpretation of the inspections and ascertaining the true state of the plant.

Keywords

Creep, Boiler, Monte Carlo, Probabilistic, Lifetime

1. Introduction

Some of the UK's Advanced Gas Cooled (AGR) reactors are already operating beyond their original design lifetime, and all the AGRs may be expected to do so in due course. At full power the reactor coolant gas temperature is around 650^{o}C as it enters the boilers. Consequently, creep is a potentially life limiting mechanism for some boiler components. The accurate prediction of creep lives is hampered by the large scatter in creep material properties. For the purposes of underwriting nuclear safety, bounding material properties are assumed in conservative assessment methodologies. The degree of conservatism in such safety related assessments can be such that, whilst entirely appropriate for ensuring safety, they give no realistic picture of plant lifetimes.

In common with boilers in conventional power plant, AGR boiler surfaces consist of large numbers of very similar tubes and associated features. This lends itself naturally to a probabilistic treatment. The failure of small numbers of tubes is tolerable from the nuclear safety perspective. Indeed the occasional occurrence of steam leaks is anticipated and managed by repairs, replacements or by plugging tubes. This need have no commercial or safety implications so long as the rate of leaks and the number of tubes requiring remediation remains small. One of the purposes of a probabilistic treatment is to predict future leak and remediation rates, and hence the likely commercial impact and the degree of challenge to the safety envelope. Two cases may be distinguished depending upon the availability of inspection evidence,

[1] Extensive in-service inspection evidence exists and there is a history of cracking as well as some steam leaks;

[2] Little or no in-service inspection evidence exists and hence the potential defectiveness is unknown other than indirectly from a few steam leaks.

Case [1] is considered in this paper. The focus in this case is on the probabilistic modelling of creep-fatigue crack growth and the probabilistic modelling of the

inspection process. Modelling the combination of these two factors statistically is unusual, though crucial to the outcome in this case.

It is intended that subsequent work will treat case [2] for which the focus will be the probabilistic modelling of either creep rupture or creep-fatigue crack initiation (possibly followed by crack growth). There is also, of course, the case where there is in-service inspection evidence but with no history of cracking. However this more benign case is unlikely to merit detailed probabilistic modelling and hence is not considered further.

2. Component Modelled

The boilers in question here are of serpentine design. The features with a known history of cracking are bifurcations in the main (superheater) boiler. These bifurcations lie at the top (the hotter end) of the boiler. They bring together the steam flows from the two tubes which comprise a single platen into a single outlet pipe, see Figure 1. In this design the swaged end of the outlet pipe is connected to the bend at the top of the platen via an oval shaped saddle weld. The boiler platen tubes are nominally 38mm OD and 4mm wall thickness. On both sides of the bifurcation the parent material is 316H stainless steel. The saddle weld is a two-pass TIG weld with compatible consumable. There are twelve boiler units per reactor, and 44 bifurcations per boiler unit, making 528 bifurcations per reactor.

Cracks have been found in the HAZ on the platen side of this saddle weld. They have been discovered centred on any of the four cardinal points shown in Figure 1, though the 0^o crotch position is most common. Cracks can occur centred on one, two, three or all four of the cardinal points, but never coalesce. The analysis and inspection results presented in this paper refer exclusively to the 0^o crotch location. Eddy current inspection is used, the results of which are expressed as percentage full-scale deflection (%FSD). One of the key features of the probabilistic simulations is to incorporate the substantial uncertainty in the conversion of %FSD to crack depth. This aspect is particularly important in the present application because of the difficulty of carrying out the inspections inside a reactor, in hot conditions with difficult access, and due to the defects being shallow.

Metallurgical examinations confirm that the crack growth mechanism is creep dominated. The mechanism which initiated the cracks, however, is less clear – partly because the initiation site has long since been consumed by oxidation. Following an increase in the incidence of reported defects in 2006 the operating temperature was reduced to ameliorate further creep degradation, specifically crack growth. At full power the bifurcations operated at typically 503^oC-525^oC. At reduced power the bifurcation temperature does not exceed 480^oC and is typically 470^oC.

3. Crack Growth Calculations

At the heart of the probabilistic simulation is a deterministic calculation of creep-fatigue crack growth. This employs volume 4/5 of EDF Energy's R5 procedure, Ref.[1]. The bifurcations have been subject to detailed finite element analyses, e.g., Ref.[2], from which the stresses used in this paper have been extracted.

Operating steam pressure at full power is ~160 barg, whereas the reactor coolant CO_2 pressure is ~40 barg, so the differential pressure is ~120 bar. The oval geometry of the branch weld results in stresses due to pressure which are substantially larger than those of the nominal tubing. In addition, the tailpipes, which convey the steam out of the reactor from the bifurcation outlets, are subject to large system loads due to boiler

thermal expansions. The combination of these two sources of stress creates an onerous condition which is probably one of the main causes of the cracking observed. (The incidence of cracking is correlated with system loading which varies across the different bifurcations in a given boiler unit). Welding residual stresses are negligible due to solution heat treatment during fabrication. However, proof testing can induce residual stresses and this was taken into account.

The fatigue contribution to crack growth is dominated by the reactor start-up/shutdown cycles. The assessments treated long shutdowns to cold conditions separately from shorter shutdowns under 'hot standby' conditions, since the latter involve much reduced system stress ranges. Reactor shutdowns can involve transient steam pressure peaks and the resulting enhanced stress ranges were included in the fatigue assessments.

The methodology involves calculating the elastic stress intensity factor (SIF) for assumed semi-elliptic cracks on the outer surface, aligned with the HAZ, characteristic of the observed defects. The calculation of fatigue crack growth is based on the SIF range via a Paris law. Creep crack growth rate is calculated using $\dot{a} = AC(t)$ where the creep fracture parameter $C(t)$ is estimated using the R5 procedure, Ref.[1] and the coefficient *A* is fitted to laboratory test data. The parameter $C(t)$ involves the SIF, the reference stress and the creep strain rate at the reference stress, amongst other factors. The use of $C(t)$ rather than C^* is to permit incorporation of secondary stresses (see Ref.[1] for details).

Crack growth is calculated at the deepest point of the semi-elliptic profile. The surface crack length, $2c$, is assumed to be related to the fractional crack depth , a/w, in a manner derived from measured crack sizes on components removed from the reactors. Hence the aspect ratio $2c/a$ is taken as 25 for very shallow defects, reducing linearly as a function of crack depth to 10 for $a/w \geq 0.63$.

4. Monte Carlo Probabilistic Simulation Methodology

The Monte Carlo method involves randomly sampling the distributed input variables many times so as to build a statistical picture of the output quantities, see for example Ref.[3]. The method has a very wide range of applicability, engineering applications being only one. The method is particularly appropriate when there are a large number of independent variables which can influence the outcome. The Monte Carlo method is being used increasingly in structural integrity applications. Examples include: applications to the analysis of creep data or the development of models of creep behaviour, e.g., Refs.[4,5,6], and in particular creep crack growth in austenitic materials, e.g., Refs.[7,8,9,10]; applications to lifetime assessment of plant components, both low temperature, e.g., Refs.[11,12], and within the creep regime, e.g., Refs.[13,14,15,16,17,18]; and applications to the evaluation or reliability analysis of non-destructive testing data, e.g., Refs.[19,20], including the development of inspection strategies and assessment of expected system availability, e.g., Refs.[21,22,23]. The present paper is perhaps unusual in applying the Monte Carlo method to structural calculations as well as inspection performance, within the same computer code, in order to predict future required remediation rates.

The particular approach to the Monte Carlo simulation in this paper is,

(i) Assume some distribution of starter crack depths immediately following initiation, as well as some distribution of initiation times (which may be at the start of life or at some time during service life);

(ii) For each of the 528 bifurcations in a given reactor, choose at random a starter crack depth and initiation time sampled from the above distributions. Similarly sample values for all the other parameters required for a structural calculation of crack growth from their assumed distributions. (The distributed variables are listed below);

(iii) Calculate the crack depth history by time-stepping numerical integration of the governing equations, and thus the predicted crack depth at the time of each inspection campaign, for all 528 bifurcations;

(iv) Using a statistical model of the inspection process and the inspection variability, sample an inspection result (%FSD) given the crack depth calculated above;

(v) Hence 'predict' a set of inspection results across the whole reactor for comparison with the inspection record for each inspection campaign;

(vi) Also, the number of defects which are calculated to grow through-wall can be compared with the history of leaks;

(vii) Tune the initiation crack depth and time distributions, (i), to optimise agreement between the 'predictions' and the plant inspection and leak history in (v) and (vi);

(viii) Use the optimised assumptions for (i) to obtain genuine predictions of future inspection results and hence the likely required level of future remediations.

The probabilistic simulation uses a Monte Carlo method with Latin Hypercube sampling, Ref.[24]. This is an efficient simulation technique which permits a large number of distributed variables to be addressed. Each variable can take one of a finite number of values each of which represents a range of values (a 'bin'). All bins are of equal probability. The Latin Hypercube algorithm ensures that all bins of all variables are sampled in the minimum number of trials (though not, of course, in all possible combinations). Moreover, because all bins are of equal probability it follows that all trials are of equal probability, thus ensuring that all trials are of equal weight in the simulation.

4.1 Distributed Structural Parameters

The parameters which are required to calculate crack growth and which are taken as distributed in the simulations are: crack initiation time, initial crack depth, tube thickness, elastic modulus, proof stress and tensile strength, creep crack growth law, creep ductility including multiaxial effects, fatigue crack growth law, operating temperature, pressure stresses, system stresses and cyclic stresses. Normal distributions are used for stresses and log-normal distributions for the other variables.

The coefficients of variation assumed for the material properties are given in Table 1, and those for illustrative stresses in Table 2 (noting that stresses vary with power level and are subject to transients during start-up and shut-down, which are also modelled). The mean operating temperature depends upon power level and differs for different reactors, lying between 509^{o}C and 529^{o}C at full power. The operating temperature was assumed to have a standard deviation of 10.6^{o}C (based on historic thermocouple data).

The creep deformation law was not taken as distributed for the final results reported here. It is known that the creep deformation rate and the creep crack growth law coefficient are inversely correlated. This follows from the known correlation between creep deformation rate and creep ductility, and the known inverse relation between creep ductility and the creep crack growth law coefficient, e.g., Refs.[4-10]. In deterministic assessments to R5, Ref.[1], this is addressed through the use of a specific set of combinations of properties. In particular, the upper bounds of both quantities are *not* considered simultaneously. In the probabilistic simulations this was crudely accounted for by fixing the creep deformation rate at its median value. This was found to produce a better fit to the plant history than if uncorrelated distributions of both creep deformation and crack growth law coefficient were employed, consistent with the evidence of correlation from laboratory creep tests. All results herein therefore relate to deformation rates fixed at their median values.

4.2 Statistical Modelling of Inspection %FSD-Crack Depth Conversion

It is crucial to appreciate that the structural calculations are only one source of uncertainty. Of equal, or greater, importance is the uncertainty in the interpretation of the inspection data. The inspection does not measure crack depth: it only provides data which are imperfectly correlated with the crack depth. The results of the eddy current inspections are reported in the form of the deflection of a needle on a dial as a percentage of the full scale deflection on the dial (abbreviated here to %FSD). Originally, this reading was calibrated against some bifurcations with machined slots to represent cracks. However, the removal of defective bifurcations from the reactors has allowed the technique to be calibrated on real cracks, resulting in recommended linear relationships between eddy current readings and best estimate and upper bound crack depths. This has been used to estimate crack depths from eddy current results, in order to decide on appropriate remedial action following inspection campaigns.

For the present purposes, however, the reverse of this procedure is required. The probabilistic code must estimate an eddy current reading given a crack depth predicted by the creep-fatigue crack growth calculation. It is important to simulate the variability in the inspection result for a given crack size. Therefore, the calibration data have been re-examined to produce a relationship between eddy current reading and crack depth. This is a refinement of the calibration line using a polynomial fit for the mean and evaluating measures of the scatter from bifurcation to bifurcation measurements and from repeat measurements on the same bifurcation.

In 2006 a more sensitive eddy current procedure was adopted. The calibration trials on ex-reactor bifurcations employed both the ‘old’ (pre-2006) and the ‘new’ (2006 and after) procedures. The Monte Carlo simulations use the appropriate fitted polynomials and errors for the time in question. Hence the sampled eddy current %FSD for a given crack depth will tend to be substantially different before and after 2006.

Figure 2a shows the ‘old’ calibration curve and its 5% and 95% confidence levels. Figure 2b shows the ‘new’ calibration curve and its 5% and 95% confidence levels. This was originally based on inspection trials in 2006. Further data obtained in 2008/9 has been added to Figure 2b. Its inclusion makes little difference to the calibration curve and confidence levels, so the calibration curve has not been refitted. Given a crack depth, these calibration curves can be used to imply the expected average %FSD of a large number of inspections on the same crack. Data in the calibration database, and also from the 2006 in-reactor inspection campaigns, for multiple

inspections on the same crack imply a standard deviation in repeat measurements of 5.9 %FSD, which is applicable to both ‘old’ and ‘new’ procedures. This was also taken into account in the Monte Carlo simulations.

4.3 Simulation of the In-Reactor Inspection Process

The methodology described in §4.2 defines how the simulation can derive a sampled eddy current %FSD for a given crack depth assuming a single measurement. However, whilst an in-reactor inspection campaign results in a single reported %FSD at a given location, this value is not necessarily derived from just one inspection, nor is each inspection result necessarily derived from just one measurement. The inspection process has changed over history, but the following gives an approximate indication based on current practice. Each inspection consists of at least two inspections by independent inspectors, and sometimes a third independent inspection. Each inspector lays the probe on the metal and takes a measurement one or more times, according to the following rules:

1. If the first measurement is greater than or equal to the recording threshold of 15%FSD the inspector makes a second measurement. Otherwise, he records “NRD” (no recordable defect) and moves on to another location.
2. If the second measurement is less than 15%FSD or the difference between the first and second measurements is greater than 10%FSD, the inspector makes a third measurement. Otherwise, the average of the first two measurements is recorded as the inspection result and the inspector moves on.
3. When three measurements are taken, NRD is recorded as the inspection result if two of them are <15%FSD, otherwise the average of the two or three results which are ≥15%FSD is reported as the inspection result.

Prior to 2008 if step 1 was NRD but inspection in an earlier year had reported a defect, the inspector was prompted to carry out a second measurement, step 2. This practice was discontinued when it was appreciated that it could bias the statistics, i.e., by increasing the likelihood of a defect being reported as a result of an earlier reported defect.

The second inspector (the verifier) repeats the above process, generally in a different reactor entry (a later shift). Prior to 2008, a second inspection was carried out only if the first inspection returned a result ≥15%FSD for the ‘old’ procedure or ≥20%FSD for the ‘new’ procedure.

Third inspections were very unusual in conjunction with the ‘old’ procedure (i.e., prior to 2006). In 2006/7, a third inspection was carried out only if the reported results of the first and second inspections differed by more than 10%FSD (using a value of 20%FSD in place of any NRD result for this purpose). Since 2008 a third inspection was also carried out if the reported result of the first or second inspection was NRD whilst the other was ≥20%FSD.

Finally it is necessary to convert the reported results of the independent inspections to just a single reported result for the inspection campaign. The rules for calculating the outcome in 2008/9 were as follows. If there were two inspections and both inspections gave values greater than 20%FSD then their average was the reported result. For two inspections, both giving NRD, then the outcome was returned as NRD. If one inspection gave NRD and the other a value less than 20%FSD, then the latter value

was returned as the outcome. If both inspections gave numerical values less than 20%FSD, then 20%FSD was returned as the outcome. If one inspection gave less than 20%FSD and the other between 20% and 30%FSD, then the average of 20%FSD and the latter value was returned as the outcome. The rules were slightly different in 2006/7. Prior to 2006 there was at most one inspection which produced a non-NRD reported result, so that was the final reported result. For 3 inspections (2008/9 onwards), NRD is returned as the outcome if two of them are NRD, otherwise the average of the two or three non-NRD results is reported.

It will be appreciated that this whole process does not lend itself to an algebraic description of the transformation from crack depth to final inspection campaign reported outcome. However, it can be simulated in the Monte Carlo programme, including its changes over the historical campaigns, by taking different random samples for each measurement (all based on the same calculated crack depth) and then combining these according to the rules given above. This is important because multiple repeat measurements can affect the statistics, as can the rules for combining them into a single reported result.

5. Results

All the results given here apply to one particular reactor and for the 0^o crotch cardinal position alone.

The first step is to tune the assumptions for the initiation crack depth distribution and the initiation time distribution to optimise agreement with the historic inspection data. Figures 3a, 3b and 3c compare the Monte Carlo 'predictions' after this tuning process with the inspection results for 24 years, 30 years and 32 years into plant life. (Note that year 30 was 2006, when the inspection procedure was changed). These histograms give the number of bifurcations returning inspection results greater than or equal to the x-value. Each Figure shows the results for median initiation times at start of life and after 10 years and 20 years. The error bars indicate the range of results from repeat Monte Carlo runs. There is little difference between the predictions for different initiation times, but these correspond to differing (optimised) assumptions for the initiation crack depth distributions. Thus, later initiation times are compensated by deeper median initiation depths. These best fit median crack depths at initiation lay between 0.52mm and 0.73mm. Note that the apparently poorer fits in Figure 3a (24 years) compared with Figures 3b,c (30 and 32 years) is simply due to the smaller numbers of bifurcations at >20%FSD in Figure 3a. The absolute differences between the fitted and actual data are comparable across all three Figures, as are the indicated error bars.

The optimised fits for the initiation depth and time also produced a prediction for the number of leaks in good agreement with the history for the reactor, though the number of leaks in question is small (3 after 17 years rising to 5 by 30 years life).

Figures 4a and 4b show the distribution of calculated crack depths across the reactor at year 30 (2006) in comparison with the start-of-life initiated distribution. In these Figures any cracked bifurcations which have actually been repaired or replaced have been retained. The in-service growth is evident. For crack sizes <1mm the three different initiation times have differing crack depth distributions at 30 years (not surprisingly since they differ at initiation). It is interesting to note, however, that for crack depths >1mm the three different initiation times correspond to very similar crack depth distributions at 30 years, as shown most clearly in Figure 4b on an

expanded scale. The reason for this is that, above the inspection threshold, the various initiation cases are all tuned to the same historic inspection data. Figure 4b also shows most clearly the importance of crack growth for the deeper defects.

Figure 4b also shows the small number of bifurcations which are predicted to have leaked by year 30 (shown at crack depths >3.3mm, at which they failed). This is an important result in that it confirms that the leaking bifurcations can arise from the same statistical population as the rest. The fact that a few bifurcations "break away" to become leakers is predicted based on the smooth, single population distributions used as input to the Monte Carlo simulations. It can be attributed to the nature of creep crack growth, with an accelerating growth rate of deep cracks under constant loading due to increasing stress intensity factor and reference stress.

Figures 4a,b do not represent the defect distributions remaining in operating tubes within the reactor. This is because the deeper defects have been removed by being remediated (i.e., repaired or replaced or taken out of service by tube plugging). Figure 5 shows the predicted defect distribution actually remaining in the reactor at times from 24 to 40 years. This illustrates the benefit of the repeated inspection campaigns in gradually removing the deeper defects. The deepest defect remaining in service at 24 years was predicted by the model to be ~2.5mm, whereas by 35 years this has reduced to ~1.55mm (despite crack growth). Note that Figure 5 is the median result of three runs of each of the three preferred fits at zero, 10 and 20 year median initiation times (9 runs in all).

Figure 6 shows the number of bifurcations requiring remediation per overhaul compared with the Monte Carlo prediction (in both cases only remediations resulting from cracks at the 0^{o} cardinal position are displayed here). The error bars indicate the range of results from repeat Monte Carlo runs (9 runs in all at each power level, as stated above for Figure 5). Up to 2006/7 (year 30) the actual remediation level is effectively part of the fitting process, rather than a prediction of the model. However, after year 30 the Monte Carlo simulations are genuine predictions of the number of required remediations. The most important feature of the simulation is the agreement with the inspection results in 2006/7 as regards the very marked increase in the number of required remediations compared with earlier years. This is in spite of the same simulations predicting only slow crack growth rates (see below and Table 3). Consequently the probabilistic simulation clearly identifies the change of inspection procedure in 2006 as being primarily responsible for the increased incidence of defects reported above the remediation threshold. This is an extremely important conclusion because it implies that the real rate of degradation of the plant was not as severe as the raw inspection results initially suggested. This conclusion is reinforced by the Monte Carlo predictions at different post-2006/7 power levels (hence different temperatures and creep rates). The predicted number of required remediations is insensitive to the power level. Nevertheless, operation at reduced power (hence reduced temperature) continues as a precaution.

Finally, Figure 6 also shows the predicted numbers of remediations for year 31 onwards. Figure 7 shows the same data in cumulative form. Inspection campaigns were carried out in years 31 and 32 and the actual remediation levels (shown as the black bars) are in good agreement with the predictions. A further important conclusion from the simulations is that a comparable, only gradually reducing, number of remediations will be required on subsequent overhauls until the end of plant life.

It is important for the integrity of the plant to ascertain the cause of the ongoing requirement for remediation. The combined statistical simulation of both the crack development and the inspection process provides evidence that the ongoing requirement for further remediations is primarily the result of the inspection variability, not of plant degradation. This conclusion follows from the good agreement between the predicted and actual remediation levels, Figures 6 and 7, despite the same simulations indicating maximum crack growth rates having reduced to almost negligible levels after power reduction, Table 3.

6. Discussion of Results

A Monte Carlo statistical treatment of both calculations of crack growth and also the in-service inspections produced results that agree well with the historical inspection and steam leak data (Figures 3a-c). This was achieved using statistical distributions of stress, material properties and inspection performance derived from data independent of the plant history. The crack depth distribution immediately post-initiation was tuned to fit the plant inspection and leak history. However it is noteworthy that the best fit median depth at initiation, 0.52-0.73mm, is consistent with evidence from metallurgical examinations.

It is not necessary to assume that there is anything different about the leaking bifurcations in order to achieve this agreement, i.e., the leaks arise from the same statistical population as the rest of the bifurcations. This is a noteworthy finding in that it can be tempting to regard a small percentage of failed components (<1% in this case) as forming a separate population, but this need not be so.

The key plant event was the marked increase in the incidence of reported defects in 2006 (Figure 6). At the time this was conservatively assumed to indicate a real rate of increase of plant degradation, and resulted in plant down-rating. However the probabilistic simulations unambiguously imply that the change of eddy current inspection procedure in 2006 was the main cause of the increased reporting of defects. This can be concluded only because the statistical errors in the inspection are included in the Monte Carlo simulations. The underlying crack depth distribution calculated in the simulations does not show any comparable sudden increase. Nevertheless, the simulations indicate that there has been sufficient growth of some of the cracks in service to be consistent with the history of leaks (Figures 4a,b).

The Monte Carlo simulations imply that maximum crack growth rates reduce by a factor of 10 or more after temperatures were reduced by $\geq 23^{o}C$ in 2007, consistent with deterministic estimates. Nevertheless the simulations predict an appreciable continuing rate of remediation to be required to the end of life (Figures 6 and 7). In fact a certain level of ‘new’ reportable defect indications is inevitable, even if there were no real change in the bifurcations, simply due to statistical variations in the inspection results. There is indeed an ongoing requirement for remediations after each inspection campaign. This might have been confused with real plant degradation. However, the fact that this was anticipated and can be understood in terms of the known inspection performance demonstrates that it is not necessarily indicative of real continuing plant degradation.

The Monte Carlo simulations give an indication of the true level of defectiveness, as opposed to that deduced directly from inspection results (Figure 5). They indicate that the inspection strategy (100% coverage at every statutory outage) is likely to have been successful in reducing the number of bifurcations with cracks deeper than the

mean detection limit (1mm), and eliminating the deepest defects which might have grown to become leakers.

7. Conclusion

Structural assessments in the creep regime are subject to large uncertainties. Difficult in-reactor inspections have limited reproducibility. A probabilistic treatment of both these issues jointly can assist in ascertaining the true state of the plant.

8. References

[1] R5, "Assessment Procedure for the High Temperature Response of Structures", R5 Issue 3, June 2003, EDF Energy. (See also D.W.Dean, P.J.Budden and R.A.Ainsworth, "R5 Procedures for Assessing the High Temperature Response of Structures: Current Status and Future Developments", Proceedings of PVP2007, the 2007 ASME Pressure Vessels and Piping Division Conference, July 22-26, 2007, San Antonio, Texas, USA, paper PVP2007-26569).

[2] D.P.Bray, R.J.Dennis and R.A.W.Bradford, "Modelling the Complex Manufacturing History of a Pipework Joint and Assessment of its Through-Life Creep-Fatigue Damage using Finite Element Based Methods", Proceedings of the ASME 2010 Pressure Vessels & Piping Division / K-PVP Conference, PVP2010, July 18-22, 2010, Bellevue, Washington, USA.

[3] D.P.Kroese, T.Taimre and Z.I.Botev," Handbook of Monte Carlo Methods", Wiley Series in Probability and Statistics, Wiley-Blackwell, April 2011.

[4] M.Yatomi and K.M.Nikbin, "Sensitivity analysis of creep crack growth prediction using the statistical distribution of uniaxial data", Fatigue & Fracture of Engineering Materials & Structures **33**, 549–561, September 2010.

[5] K.M.Nikbin, M.Yatomi, K.Wasmer and G.A.Webster, "Probabilistic Analysis of Creep Crack Initiation and Growth in Pipe Components", Int.J.Press.Vess.& Piping **80**, 585-595, July-August 2003.

[6] W.G.Kim, J.Y.Park, S.D.Hong and S.J.Kim, "Probabilistic assessment of creep crack growth rate for Gr.91 steel", Nuclear Engineering and Design **241**, 3580-3586, Sept.2011.

[7] K.Wasmer, K.M.Nikbin and G.A.Webster, "Prediction of Scatter in Creep Crack Growth Data from Creep Failure Strain Properties", ASTM International Standards, STP480-EB (*Fatigue and Fracture Mechanics*), Jan.2007.

[8] W.G.Kim, S.N.Yoon, W.S.Ryu, S.J.Kim and W.Yi, "Probabilistic Analysis of the Creep Crack Growth Rate of Type 316LN Stainless Steel by the Monte Carlo Simulation", Journal of ASTM International **3**, 3375-3384, Jan.2006.

[9] J.T.Gliniak, D.G.Harlow and T.J.Delph, "A probabilistic model for the growth of creep cracks", Engineering Fracture Mechanics **57**, 25-39, May 1997.

[10] T.Kitamura and R.Ohtani, "Creep Life Prediction Based on Stochastic Model of Microstructurally Short Crack Growth", NASA Technical Memorandum 100245, June 1988.

[11] S.Rahman, N.Ghadiali, G.M.Wilkowski and D.Paul, "A computer model for probabilistic leak-rate analysis of nuclear piping and piping welds", Int.J.Press.Vess.& Piping **70**, 209-221, March 1997.

[12] J.Rajasankar, N.R.Iyer and T.V.S.R.Appa Rao, "Structural integrity assessment of offshore tubular joints based on reliability analysis", Int.J.Fatigue **25**, 609-619, July 2003.

[13] T.J.Delph, D.L.Berger, D.G.Harlow and M.Ozturk, "A Probabilistic Life Prediction Technique for Piping Under Creep Conditions", J.Press.Vess.Tech **132**, 051206, Oct.2010.

[14] J.Zhao, D.M.Li, J.S.Zhang,W.Feng and Y.Y.Fang, "Introduction of SCRI model for creep rupture life assessment", Int.J.Press.Vess.& Piping **86**, 599-603, Sept.2009.

[15] H.Deschanels, C.Escaravage, N.Le Mat Hamata and D.Colantoni, "Assessment of industrial components in high temperature plant using the ALIAS-HIDA – A case study", Engineering Failure Analysis **13**, 767-779, July 2006.

[16] C.Zhou and S.Tu, "A stochastic computation model for the creep damage of furnace tube", Int.J.Press.Vess.& Piping **78**, 617-625, Sept.2001.

[17] R.K.Penny and M.A.Weber, "Robust methods of life assessment during creep", Int.J.Press.Vess.& Piping 50, 109-131, 1992.

[18] D.Hu and R.Wang, "Probabilistic Analysis on Turbine Disk Under LCF-Creep", ASME Conference *Turbo Expo 2008: Power for Land, Sea and Air* (GT2008), June 9-13, Berlin; Volume 5: Structures and Dynamics.

[19] I.K.Park and H.M.Kim, "Reliability Assessment of Ultrasonic Nondestructive Inspection Data Using Monte Carlo Simulation", American Institute of Physics Conference Review of Progress in Quantitative Nondestructive Evaluation, 14-19 July 2002, AIP Proceedings **657**, 1854-1861.

[20] A.Walker, W.Daniels and S.Wedge "Use of Monte-Carlo Methods to Derive Quantitative Probability of Defect Detection Data", 4th European-American Workshop on Reliability of NDE, Federal Institute for Materials Research and Testing (BAM), Berlin 24-26 June 2009.

[21] A.C.Marquez, A.S.Heguedas and B.Iung, "Monte Carlo-based assessment of system availability. A case study for cogeneration plants", Reliability Engineering & System Safety **88**, 273-289, 2005.

[22] Y.Kleiner, "Scheduling inspection and renewal of large infrastructure assets", J.Infrastructure Systems **7**, 136-143, Dec.2001.

[23] B.N.Leis and S.Rahman, "Risk-Based Considerations in Developing Strategies to Ensure Pipeline Integrity – Part 1: Theory", Trans. ASME **116**, 278, Aug.1994.

[24] M.D.McKay, R.J.Beckman and W.J.Conover, "A Comparison of Three Methods for Selecting Values of Input Variables in the Analysis of Output from a Computer Code", Technometrics (American Statistical Association) **21**, 239–245, May 1979.

Table 1 Distributed Material Properties and their Coefficients of Variation

Type	Property	CoV
Elastic	Young's Modulus	$\approx 0.038^{\$}$
Plastic	0.2% Proof Stress	$\approx 0.23^{\$}$
	1% Proof Stress	$\approx 0.23^{\$}$
	UTS	$\approx 0.11^{\$}$
	Strain at UTS	$\approx 0.18^{\$}$
Creep	Deformation Law	1.765 (Primary)[#] 1.648 (Secondary)[#]
	Ductility	$\approx 0.8^{\$}$
	Crack Growth Law	0.61
Fatigue	Crack Growth Law 'A' Parameter	3.56

$^{\$}$signifies exact value is temperature dependent
#only used in a sensitivity study (main results use mean deformation)

Table 2 Illustrative Stresses and their Coefficients of Variation
(Normal operation at 100% power)

Condition	Mean Membrane (MPa)	Mean Bending (MPa)	CoV
Pressure Stress	48.4	25.9	0.15
System Stress	19.5	14.7	0.969
Hot-Cold Stress Range	84.2	50.4	0.293

Table 3 **Predicted Maximum Crack Growth Rate for Any Bifurcation**
Expressed as % of the remaining ligament/year, the 'Greatest' and 'Median' values are evaluated over 36 Monte Carlo runs over all 528 bifurcations per reactor at 100% power, and 9 runs for each of 70% and 80% power. In all cases only the maximum growth rate for any of the 528 bifurcations is retained (not counting those remediated).

	Inspection Time								
	Pre-Power Reduction					**Post-Power Reduction**			
	20yrs	**22yrs**	**24yrs**	**29yrs**	**30yrs**	**31yrs**	**32yrs**	**35yrs**	**40yrs**
	100% Power					**70% Power**			
Greatest	29	37	39	18	79	0.90	0.81	0.31	0.31
Median	8.0	7.2	5.7	3.0	4.1	0.07	0.07	0.07	0.07
						80% Power			
					Greatest	1.57	1.65	1.79	2.03
					Median	0.20	0.21	0.21	0.22

Figure 1: Bifurcation Geometry and Potential Crack Positions

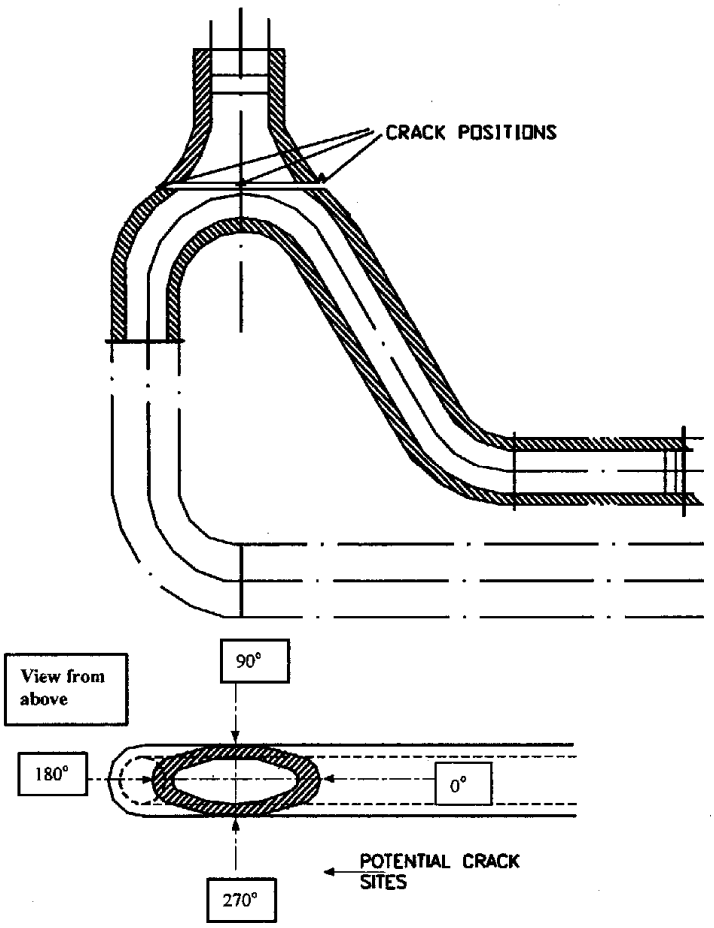

Figure 2a: Calibration Curve for 'Old' Inspection Procedure (data points are means of several measurements on the same crack)

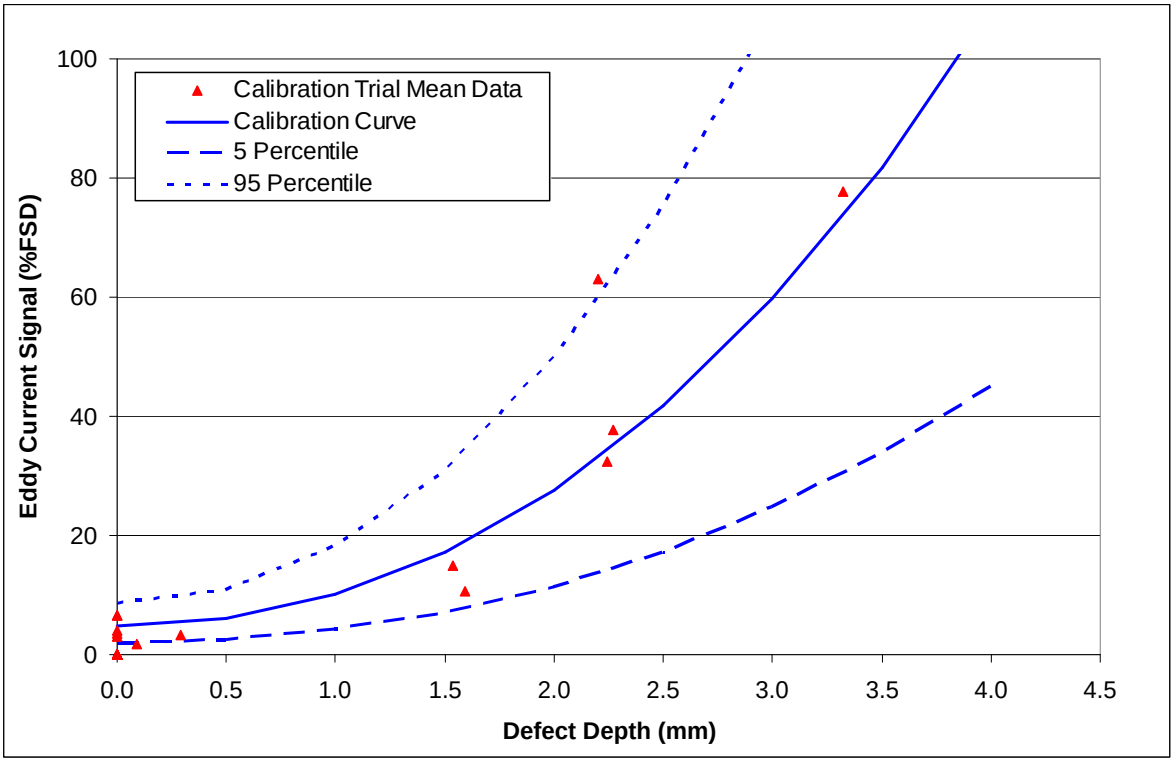

Figure 2b: Calibration Curve for 'New' Inspection Procedure (data points are means of several measurements on the same crack)

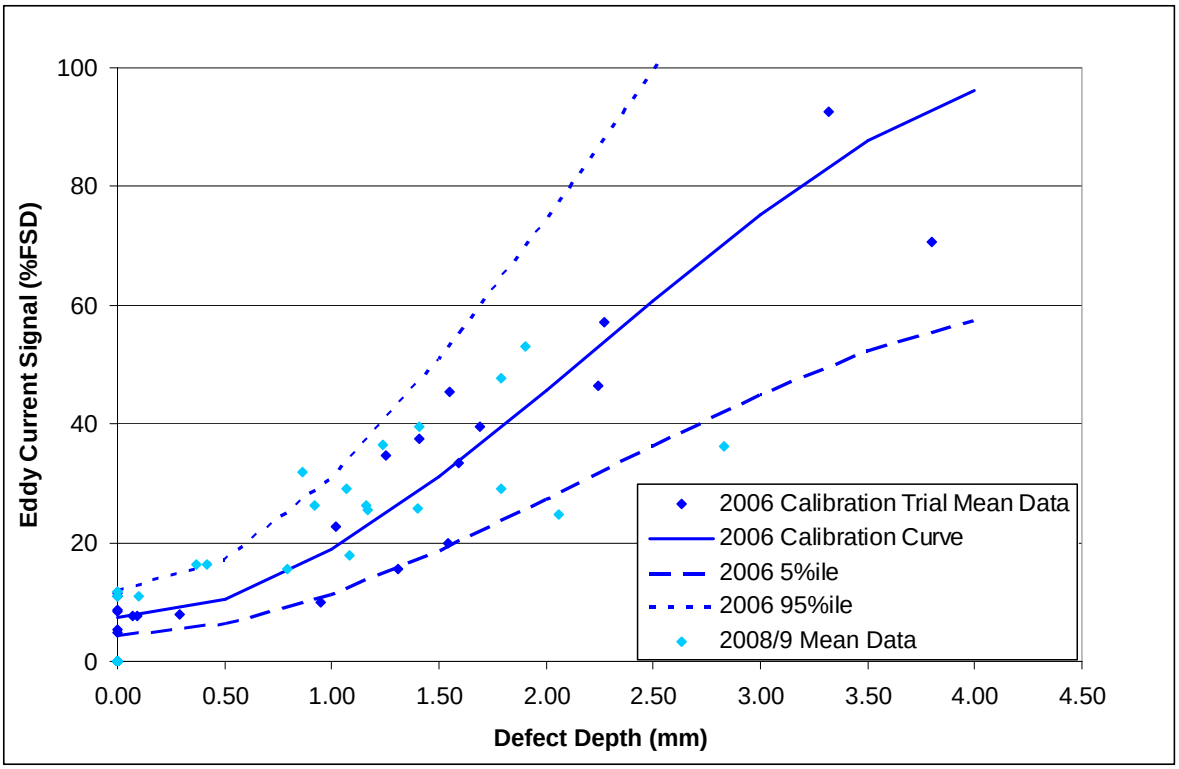

Figure 3a: Comparison of Fitted and Actual Inspection Results at 24 Years (number of bifurcations exceeding each plotted eddy current signal level)

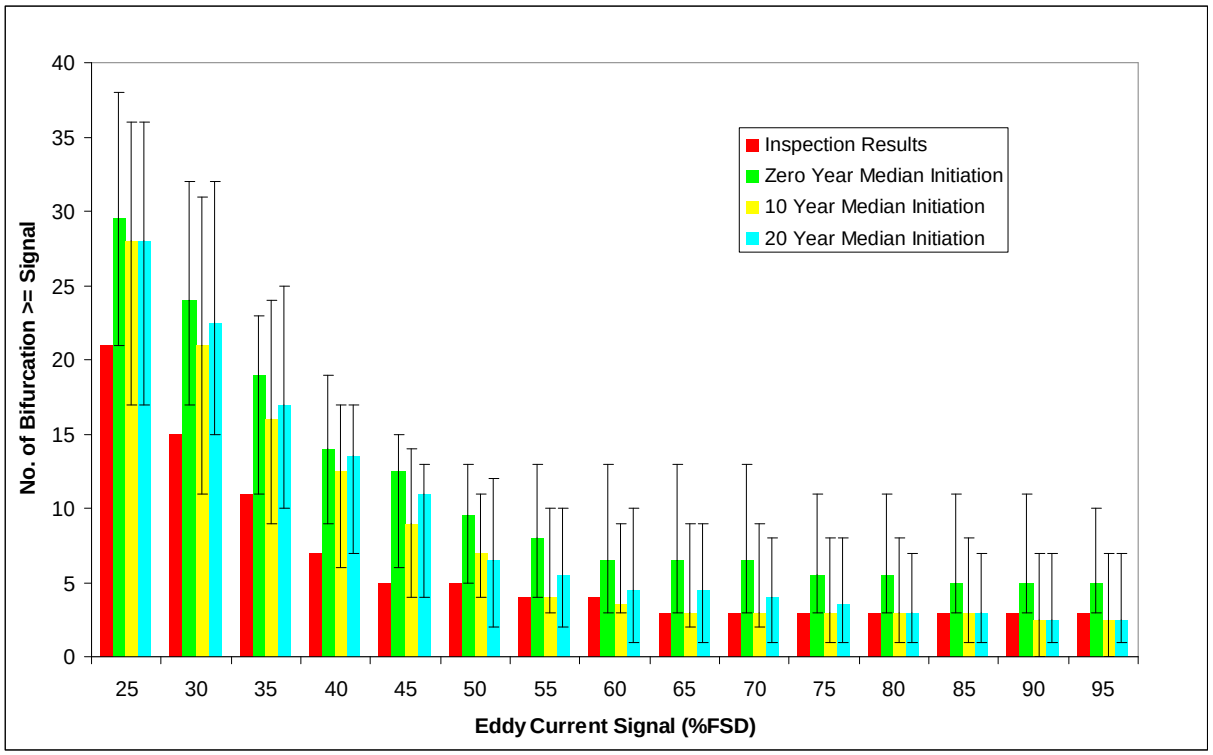

Figure 3b: Comparison of Fitted and Actual Inspection Results at 30 Years (number of bifurcations exceeding each plotted eddy current signal level)

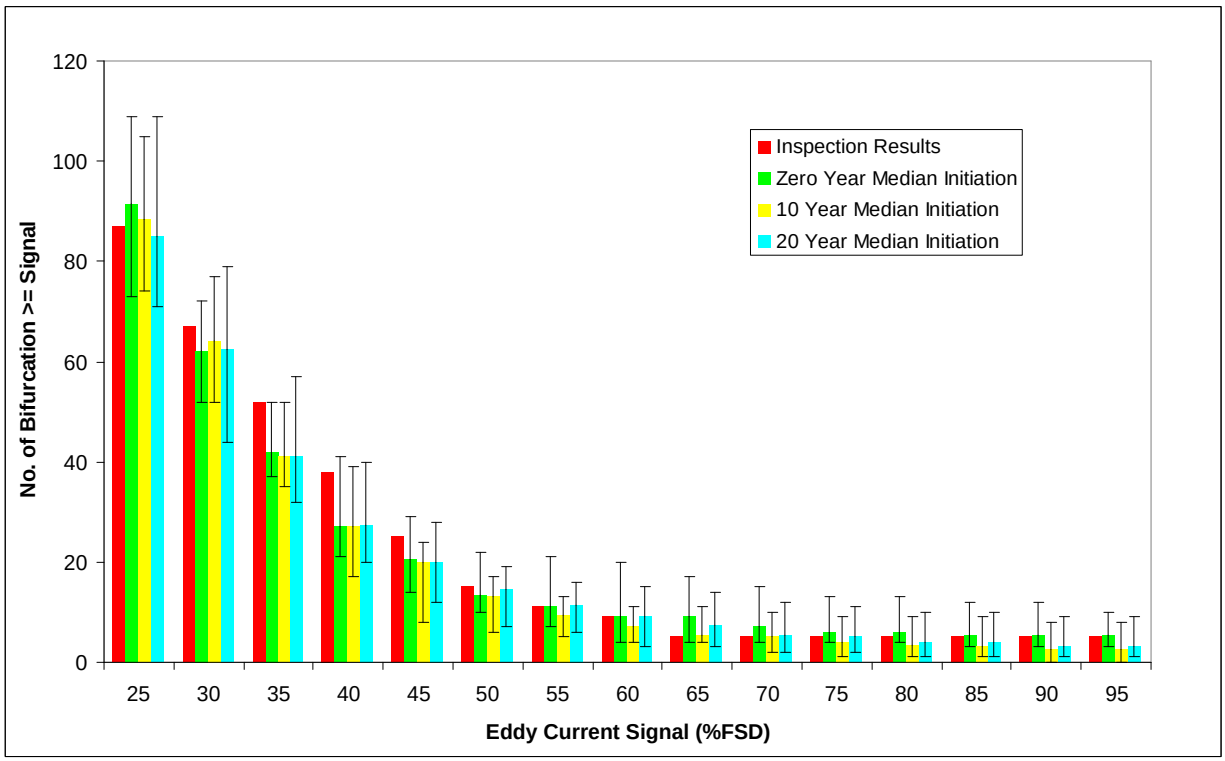

Figure 3c: Comparison of Fitted and Actual Inspection Results at 32 Years (number of bifurcations exceeding each plotted eddy current signal level)

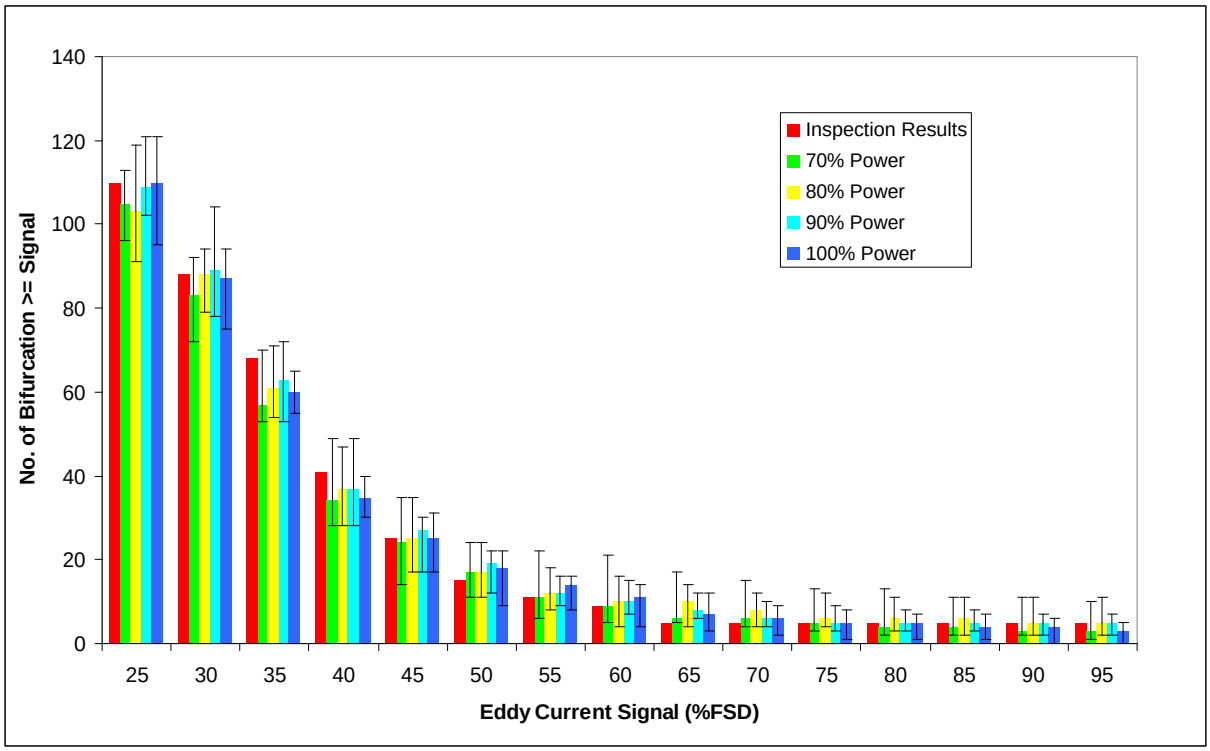

Figure 4a: Distribution of Simulated Crack Depths at 30 Years, including previously remediated and leaking bifurcations. Illustrates the modelled crack growth.

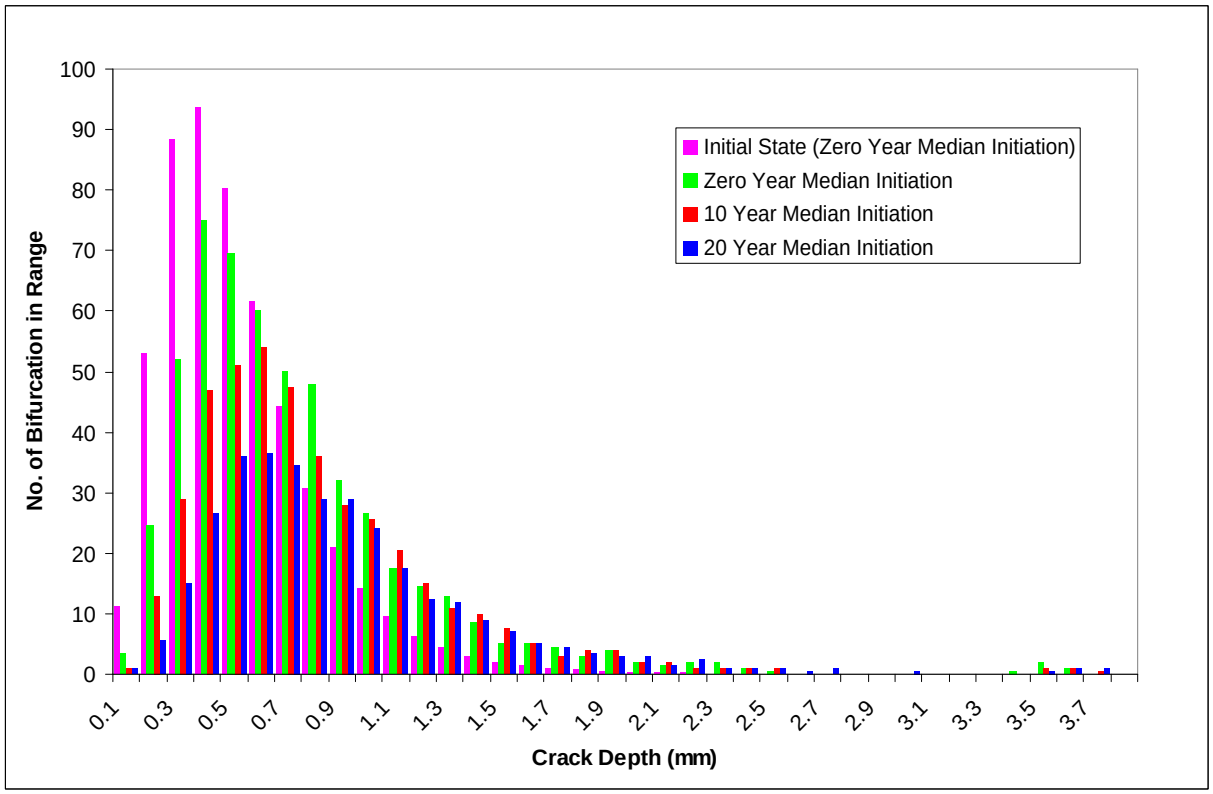

Figure 4b: Distribution of Simulated Crack Depths at 30 Years, including previously remediated and leaking bifurcations (expanded scale for depths >1mm). Illustrates the modelled crack growth and the occurrence of leaks (right-most cracks)

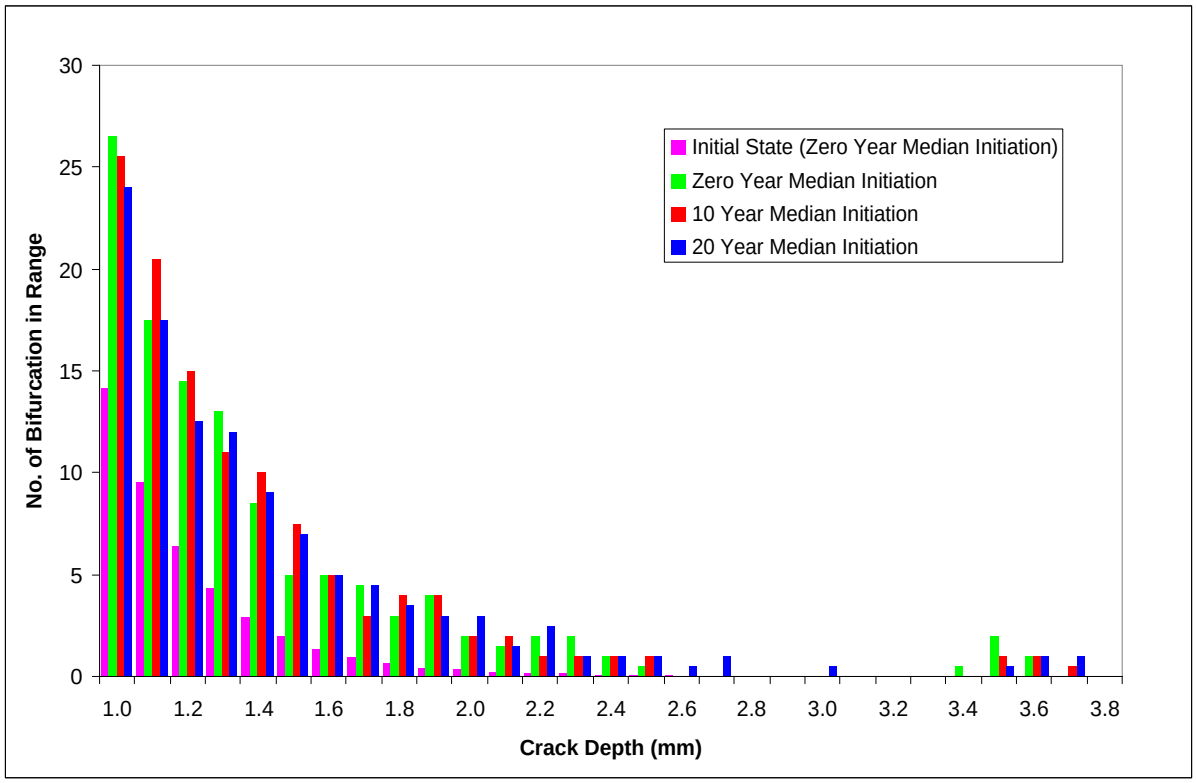

Figure 5: Distribution of Crack Depths between 24 and 40 Years, excluding remediated and leaking bifurcations. Illustrates removal of the deeper cracks.

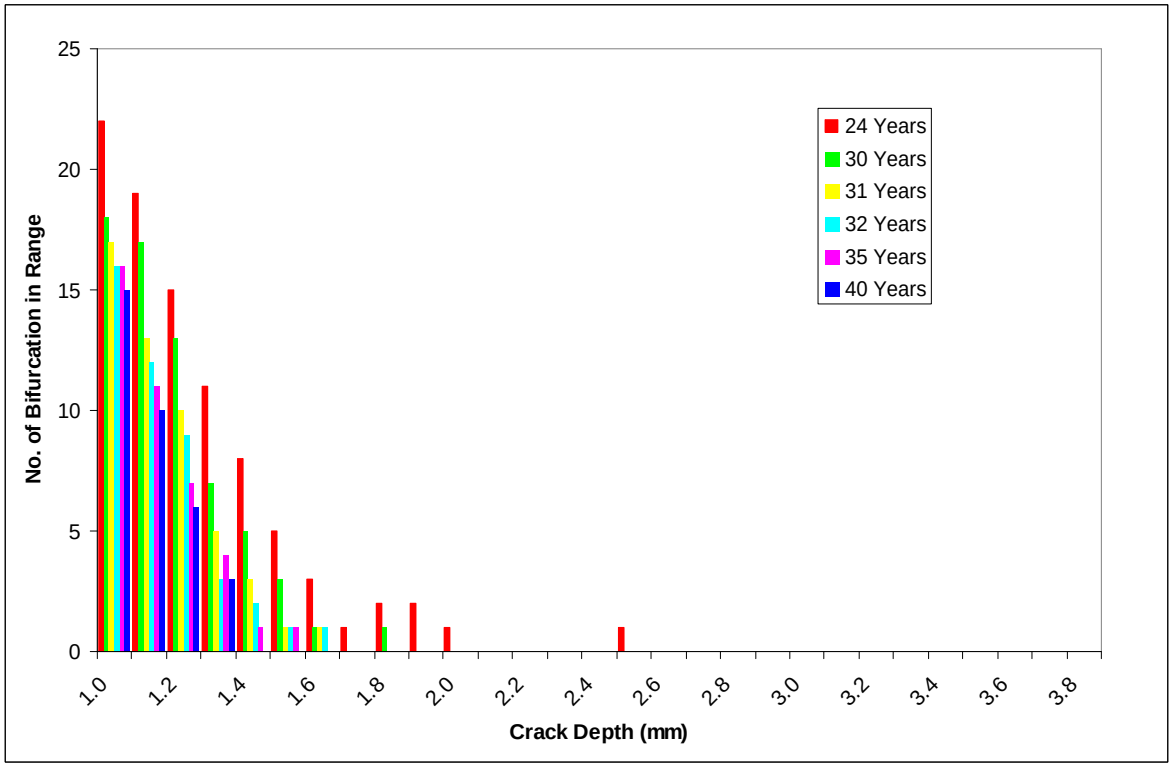

Figure 6: Comparison of Predicted and Actual Number of Remediations by Year

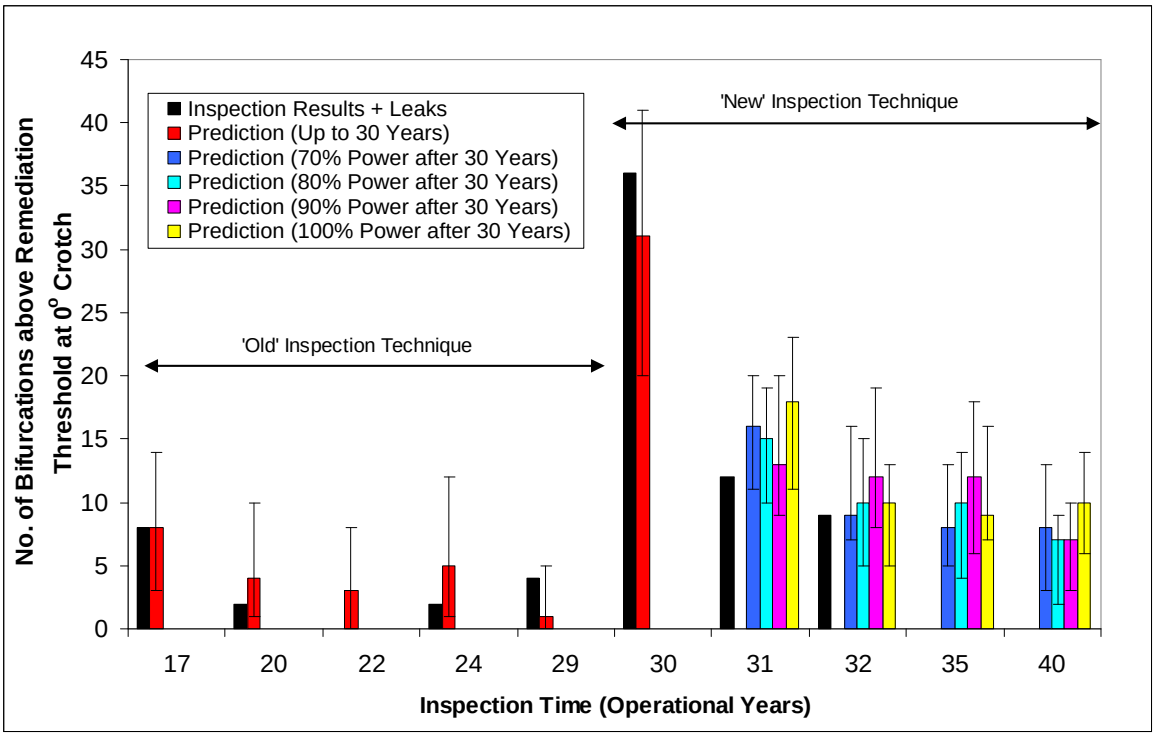

Figure 7: Comparison of Predicted and Actual Number of Remediations (Cumulative)